FULL PAPER

Dalton
www.rsc.org/dalton

Hydrothermal synthesis and crystal structure of two Co phosphonates containing trifunctional phosphonate anions: $Co_3(O_3PCH_2NH_2CH_2PO_3)_2$ and $Co_3(O_3PCH_2\text{-}NC_4H_7\text{-}CO_2)_2\cdot 5H_2O$

Adele Turner,[a] Paul-Alain Jaffrès,[b] Elizabeth J. MacLean,[c] Didier Villemin,[b] Vickie McKee[d] and Gary B. Hix *[a]

[a] *Department of Chemistry, De Montfort University, The Gateway, Leicester, UK LE1 9BH. E-mail: ghix@dmu.ac.uk*

[b] *LCMT, UMR CNRS 6507, Ecole Nationale Supérieure d'Ingénieur de Caen, Université de Caen, ISMRA, 6 Bd du, Maréchal Juin, F-14050 Caen, France*

[c] *CLRC Daresbury Laboratory, Daresbury, Warrington, Cheshire, UK WA4 4AD*

[d] *Chemistry Department, Loughborough University, Loughborough, UK LE11 3TU*

Received 13th December 2002, Accepted 10th February 2003
First published as an Advance Article on the web 25th February 2003

Two cobalt phosphonates containing trifunctional phosphonate anions have been synthesised and their structures solved by single crystal diffraction. $Co_3(O_3PCH_2NH_2CH_2PO_3)_2$ (**3**) was formed as blue crystals. The material has three channel systems in the [001] direction formed by the cross-linking of chains of tetrahedrally co-ordinated Co atoms. $Co_3(O_3PCH_2\text{-}NC_4H_7\text{-}CO_2)_2\cdot 5H_2O$ (**4**), which contains anions derived from proline, was formed as purple crystals. (**4**) is composed of layers that contain holes. The layers stack in the [001] direction such that channels are formed in the same direction, in which the water molecules are located.

Introduction

Metal phosphonates have received a great deal of attention over the last ten years. As a class of material they have been known for around 25 years,[1] but in recent years the possibilities they present in terms of porous, functionalised materials has made them very attractive for a number of potential applications.

Until the advent of the first porous phosphonates in 1994[2] the development of this aspect of phosphonate chemistry was largely unstudied. A few reports had appeared in the literature discussing attempts at forming porous materials using diphosphonates, the results of which were not particularly encouraging, since in most cases when porosity was achieved the materials were mesoporous though without uniform or well defined pores.[3–5]

Since 1994 it has been realised that the use of bifunctional phosphonate anions (containing a functional group in addition to the $-PO_3$ group) can lead to bonding modes conducive to pore formation. Carboxylate and carboxylic acid groups have proved to be particularly efficient in this respect and phosphonoacetates, as they are known, of many transition and main group metals have been reported in the literature.[6–14] In these materials one of the oxygen atoms of the carboxylate group acts as a Lewis base and co-ordinates to the metal atoms. The resulting structure depends upon the size and rigidity of the chain linking the carboxylate and the phosphate ($-PO_3^{2-}$) group.

Other functional groups that have shown the same properties are hydroxyl,[15,16] amine[17] and amide[16] groups.

What most of these materials have in common is that once the second functional group is involved in co-ordinating to the metal atoms, the functionality that it brings to the material is lost. A logical solution to this is to increase the number of functional groups in the phosphonate anion. It has been shown using amino acid-containing phosphonate anions that the phosphate and carboxylate groups co-ordinate to the metal atoms, leaving the amine free in the pores.[10] In this paper we report our attempts at using trifunctional phosphonate anions in the synthesis of porous functionalised materials; $[O_3PCH_2\text{-}NC_4H_8\text{-}CO_2]^{3-}$, a derivatised proline molecule, and $[O_3PCH_2\text{-}NH_2CH_2PO_3]^{3-}$, a diphosphonate containing a protonated secondary amine group.

Experimental

Synthesis of $HO_3PCH_2NH_2CH_2PO_3H_2$ (1)

This compound, now commercially available, was obtained as the main product of a Moedritzer–Irani reaction[18] using (±)-phenylethyl-1-amine as the substrate (during the course of the reaction a C–N bond is cleaved): 133 mmol of formaldehyde (37% in water, 10 ml) was added in 15 minutes to a solution of 33 mmol of (±)-phenylethyl-1-amine (4.0 g), 66 mmol of phosphorous acid (5.42 g) in and 10 ml of hydrochloric acid (6.5 M in water). The solution was heated under microwave for 15 minutes at 240 W. The solution was extracted with diethyl ether. The aqueous phase was concentrated *in vacuo* to yield a white solid. Recrystallisation in ethanol yields compound (**1**) (2.95 g) as a white solid. δ_H (400 MHz, D_2O): 43.2 (dd, $^1J_{CP}$ = 140.6, $^3J_{CP}$ = 6.5 Hz); δ_P (161.9 MHz, D_2O): 8.07.

Synthesis of (*S*)-$HO_3PCH_2\text{-}NHC_4H_7\text{-}CO_2H$ (2)

This compound was synthesised using a modification of the literature method:[19] 13 mmol (1.51 g) of L-proline, 26 mmol (2.13 g) of phosphorous acid and 4 ml of hydrochloric acid (6.5 M in water) were placed in a round bottom flask fitted with a reflux condenser and heated for 5 minutes using a heating mantle. 54 mmol (1.5 ml) of formaldehyde (36% aqueous solution) was added. The solution was further heated at reflux for 90 minutes. Water was removed *in vacuo*, then 30 ml of ethanol was added. The solution was refluxed leading to the formation of a white solid. This solid was recovered by filtration, dried *in vacuo* to yield compound (**2**) (2.12 g, 78%). $[\alpha]_D = -96°$ (*c* 3.82 mg ml^{-1}, water 20 °C, path length: 10 cm); δ_H (400 MHz, D_2O + Na_2CO_3): 1.91–2.42 (m, 4H), 3.26 (m, $^2J_{PH}$ = 11.5 Hz, 2H), 3.49 (m, 1H), 3.85 (m, 1H), 4.07 (dd, $^3J_{HH}$ = $^3J_{HH}$ = 6.58 Hz, 1H); δ_C (100.6 MHz, D_2O + Na_2CO_3): 23.42, 28.68, 51.95 (d, $^1J_{CP}$ = 136.2, N–CH_2–P), 56.55, 71.73, 173.85 (s, COOH); δ_P (161.9 MHz, D_2O + Na_2CO_3): 8.02.

Synthesis of Co phosphonates

Synthesis of $Co_3(O_3PCH_2NH_2CH_2PO_3)_2$ (3). 1.83 mmol (0.455 g) of $Co(CH_3CO_2)_2\cdot 4H_2O$ was dissolved in 10 ml distilled water. To this solution was added 1.27 mmol (0.261 g)

DOI: 10.1039/b212266a

of **1**. The solution was then stirred for 10 minutes before the resulting mixture was placed in a Teflon lined stainless steel autoclave, which has a capacity of 23 ml. The reaction mixture was heated under autogeneous pressure at 433 K for a period of 48 hours, after which it was removed from the oven and allowed to cool. The blue crystalline product was recovered by filtration and washed with distilled water before drying at room temperature (Yield: 0.322 g, 91% based on Co. Found: C, 8.37; H, 1.97; N, 4.82%. Calculated: C, 8.27; H, 2.08; N, 4.83%).

Synthesis of $Co_3(O_3PCH_2\text{-}NC_4H_7\text{-}CO_2)_2\cdot 5H_2O$ (4). 1.83 mmol (0.455 g) of $Co(CH_3CO_2)_2\cdot 4H_2O$ was dissolved in 10 ml distilled water. To this solution was added 1.83 mmol (0.380 g) of **2**. The solution was then stirred for 10 minutes before the resulting mixture was placed in a Teflon lined stainless steel autoclave, which has a capacity of 23 ml. The reaction mixture was heated under autogeneous pressure at 433 K for a period of 48 hours, after which it was removed from the oven and allowed to cool. The purple crystalline product was recovered by filtration and washed with distilled water before drying at room temperature (Yield: 0.369 g, 89% based on Co. Found: C, 21.18; H, 4.22; N, 4.33%. Calculated: C, 21.16; H, 4.11; N, 4.44%).

Sample characterisation

CHN contents were determined using a Carlos Elba 1108 analyser.

Single crystal diffraction

Both samples were examined under a microscope and in the case of $Co_3(O_3PCH_2\text{-}NC_4H_7\text{-}CO_2)_2\cdot 5H_2O$, this inspection revealed the presence of only very small (dimensions in the region of 10 μm) single crystals. These crystals were investigated using microcrystal diffraction facilities at Daresbury SRS.[20] A laboratory instrument was employed for the larger crystals of $Co_3(O_3PCH_2NH_2CH_2PO_3)_2$.

Laboratory data acquisition. Crystallographic data for **3** were collected at 150(2) K on a Bruker SMART 1000 diffractometer using Mo-Kα radiation (λ = 0.71073 Å). The structure was solved by direct methods and refined by full-matrix least-squares on F^2 using the SHELXTL[21] package. The structure was refined as a racemic twin with additional disorder involving Co2 and P2, which were refined with occupancy ratio of 84 : 16 for the major and minor sites, respectively. All non-hydrogen atoms were refined with anisotropic atomic displacement parameters except for the minor components of the disorder, and hydrogen atoms were inserted at calculated positions.

Synchrotron microcrystal diffraction data acquisition. Data were collected at low temperature (150 K) using a Bruker AXS SMART CCD area-detector diffractometer on the high-flux single crystal diffraction station 9.8 at the CLRC Daresbury Laboratory Synchrotron Radiation Source, Cheshire, UK. The experiments used X-rays of wavelength 0.6877 Å selected by a horizontally focusing silicon (111) monochromator and vertically focused by a cylindrically bent palladium-coated zerodur mirror. The data set covered a hemisphere of reciprocal space with several series of exposures. Corrections were made for the synchrotron beam intensity decay as part of the standard inter-frame scaling procedures. An empirical absorption correction was applied to the data using the SADABS program.[22]

Structure solution was carried out by direct methods using the SHELXS program[23] (employed within the WINGX suite of programs[24]) and revealed the location of all non-hydrogen atoms, which were refined anisotropically. The H atoms were typically either located in the Fourier difference map or placed geometrically. Subsequent refinement of the displacement parameters of the hydrogen atoms was carried out isotropically in all cases. The hydrogen atoms of the water molecules were not located in the solution or the subsequent refinement of the structure.

CCDC reference numbers 199769 and 199770.

See http://www.rsc.org/suppdata/dt/b2/b212266a/ for crystallographic data in CIF or other electronic format.

Table 1 Crystallographic data for $Co_3(O_3PCH_2NH_2CH_2PO_3)_2$ (**3**) and $Co_3(O_3PCH_2\text{-}NC_4H_7\text{-}CO_2)_2\cdot 5H_2O$ (**4**)

Sample	**3**	**4**
Empirical formula	$C_2H_6Co_{1.50}NO_6P_2$	$C_{12}H_{28}Co_3O_{15}N_2P_2$
M	290.41	679.02
Crystal system	Orthorhombic	Triclinic
Space group	$P2_12_12$ (no. 18)	$P\bar{1}$ (no.2)
a/Å	10.733(3)	9.9849(24)
b/Å	13.387(4)	10.3782(26)
c/Å	5.3953(13)	11.9419(29)
α/°	90	90.238(5)
β/°	90	106.810(5)
γ/°	90	111.346(4)
V/Å^3	775.31(4)	1095.00(30)
Z	4	2
T/K	150	150
μ/mm^{-1}	3.650	2.472
Independent reflections	1840	3736
R_{int}	0.039	0.076
Observed reflections	1585	2475
R_1	0.0404	0.054
wR_2	0.0896	0.122
R_1 (all data)	0.0516	0.095
wR_2 (all data)	0.0946	0.138

Results and discussion

Structure of $Co_3(O_3PCH_2NH_2CH_2PO_3)_2$

$Co_3(O_3PCH_2NH_2CH_2PO_3)_2$† crystallises in the spacegroup $P2_12_12$ (no. 18) with the cell parameters given in Table 1. Bond lengths and angles are given in Table 2. The structure is three-dimensional and is based on cross-linked chains of Co atoms.

Structural analysis reveals that the material has a Co : phosphonate ratio of 3 : 2. It is also clear that the diphosphonate anions are deprotonated and hence each $-PO_3$ group carries a nominal 2− charge. Valence bond calculations, based on the method of Brown and Altermatt[25] were carried out, which yielded values of 1.948 and 1.980 for Co(1) and Co(2) respectively confirming that both Co atoms are in the +2 oxidation state. The only way in which neutrality of the material can be achieved is by considering the possibility that the secondary amine is protonated. The structure was solved with and without the additional proton, and the fit including the $-NH_2-$ group was marginally better than that containing –NH–.

The material contains two crystallographically distinct Co atoms in slightly distorted, tetrahedral co-ordination environments with Co–O bond lengths in the range 1.937(4)–1.985(4) Å. Both P atoms of the diphosphonate anions are also tetrahedrally coordinated with P–O bond lengths in the range 1.488(5)–1.524(4) Å. Each chain in the structure contains a repeating 'figure-of-eight' motif containing 3 Co atoms (Fig. 1). The Co(2) atom at the centre of this motif, lies on the two-fold axis which runs in the c-direction and is linked to the two, symmetry-related Co(1) atoms through one of the O_3P groups of the diphosphonate anion. The other end of the anion

† All atoms in (**4**) were well behaved. Disorder problems exist for (**3**). An ordered model gave rise to two large residuals of 6.86 e Å^3 and 2.84 e Å^3, which were 2.02 Å and 0.76 Å from Co2 and P2 respectively. The R_1(obs) for this fit was 6.9%. These peaks were assigned as Co2′ and P2′ and the occupancies of Co2, Co2A, P2 and P2A allowed to refine. The occupancies of Co2A and P2A were found to be approximately 16%, and R_1(obs) was reduced to 4.12%. The largest remaining featureless residual peak was now 1.086 e Å^3. Analysis of the residual peaks failed to locate disordered peaks of other atoms present in the ordered model.

Table 2 Bond lengths [Å] and angles [°] for $Co_2(O_3PCH_2NHCH_2PO_3)_2$

Co1–O3[a]	1.940(5)	Co2–O4[d]	1.937(4)
Co1–O5	1.945(4)	Co2–O4[b]	1.937(4)
Co1–O2[b]	1.964(5)	Co2–O1[d]	1.967(4)
Co1–O6[c]	1.985(4)	Co2–O1[b]	1.967(4)
P1–O3	1.488(5)	P2–O6	1.510(5)
P1–O1	1.503(4)	P2–O5	1.514(4)
P1–O2	1.524(4)	P2–O4	1.516(4)
P1–C2	1.797(6)	P2–C1	1.841(6)
N1–C1	1.508(7)	N1–C2	1.495(7)
O3[a]–Co1–O5	115.2(2)	O2–P1–C2	107.5(3)
O3[a]–Co1–O2[b]	108.7(2)	O6–P2–O5	110.1(2)
O5–Co1–O2[b]	112.4(2)	O6–P2–O4	113.4(2)
O3[d]–Co1–O6[c]	108.7(2)	O5–P2–O4	114.9(2)
O5–Co1–O6[c]	112.5(2)	O6–P2–C1	104.7(3)
O2[b]–Co1–O6[c]	97.96(18)	O5–P2–C1	107.5(3)
O4–Co2–O4[e]	116.3(3)	O4–P2–C1	105.6(3)
O4–Co2–O1[d]	111.78(16)	P2–O4–Co2	136.8(3)
O4[e]–Co2–O1[d]	108.64(17)	P2–O5–Co1	136.6(2)
O4–Co2–O1[a]	108.64(17)	P2–O6–Co1	135.4(3)
O4[e]–Co2–O1[b]	111.78(16)	C2–N1–C1	114.2(5)
O1[d]–Co2–O1[b]	98.3(3)	P1–O1–Co2	147.4(3)
O3–P1–O1	115.3(3)	P1–O2–Co1[f]	126.6(3)
O3–P1–O2	110.7(3)	P1–O3–Co1[g]	142.4(3)
O1–P1–O2	111.8(3)	N1–C1–P2	116.2(4)
O3–P1–C2	105.3(3)	N1–C2–P1	111.9(4)
O1–P1–C2	105.6(3)		

Symmetry operations for equivalent atoms: a $-x + 1/2, y - 1/2, -z + 2$; b $-x + 1/2, y - 1/2, -z + 1$; c $x + 1/2, -y + 1/2, -z + 1$; d $x - 1/2, -y + 1/2, -z + 1$; e $-x, -y, z$; f $-x + 1/2, y + 1/2, -z + 1$; g $-x + 1/2, y + 1/2, -z + 2$.

performs a similar function in a neighbouring chain in the structure, thereby linking chains to one another *via* a $–CH_2NH_2CH_2–$ covalent bridge. The chains are further linked to one another *via* Co–O–P bridges as the $–PO_3$ groups link to Co atoms in different chains. The arrangement is shown schematically in Fig. 1(b).

The result of cross-linking chains in this manner is the formation of three channel systems that are parallel to one another and run in the *c* direction (Fig. 2). The largest of the three channel systems (A) has a window made up of 12 atoms. The dimensions of this channel are difficult to define due to the irregular shape, but the longest distance between atoms in the window is *ca.* 5.9 Å (O4–C1) and the shortest is *ca.* 3.2 Å (C2–O5) (Fig. 2). The next channel system (B) has a window formed from eight atoms and has an elongated hexagonal shape. The dimensions of this channel are *ca.* 3.4 Å (O1–O5) × 4.6 Å (O2–P2). The last channel system (C) has the largest number of atoms (sixteen) forming the window, but has the smallest effective opening. This ring of 16 atoms is folded into a 'boat-like' conformation, rather than being planar. Hence the effective dimensions of the channel are *ca.* 2.7 Å (C1–O2) × 3.4 Å (O2–O2_2).

The smallest channel is the one that is of most interest with respect to potential applications. This is due to the fact that the protonated amine groups are to be found in this channel with the N–H bonds being directed into the channel void. Equivalent hydrogen atoms on neighbouring nitrogen atoms are approximately 5.4 Å apart in the [001] direction. The presence of a charge balancing proton located inside one of the channels opens up the possibility of applications in ion exchange or ionic transport, though the latter may be hindered somewhat by the large distance between sites.

The composition of $Co_3(O_3PCH_2NH_2CH_2PO_3)_2$ derived from the single crystal data analysis is consistent with the CHN analysis results of the bulk sample (see Experimental section).

Structure of $Co_3(O_3PCH_2\text{-}NC_4H_7\text{-}CO_2)_2\cdot 5H_2O$

Analysis of the single crystal data reveals that this material crystallises in the triclinic spacegroup $P\bar{1}$ (no. 2) with cell

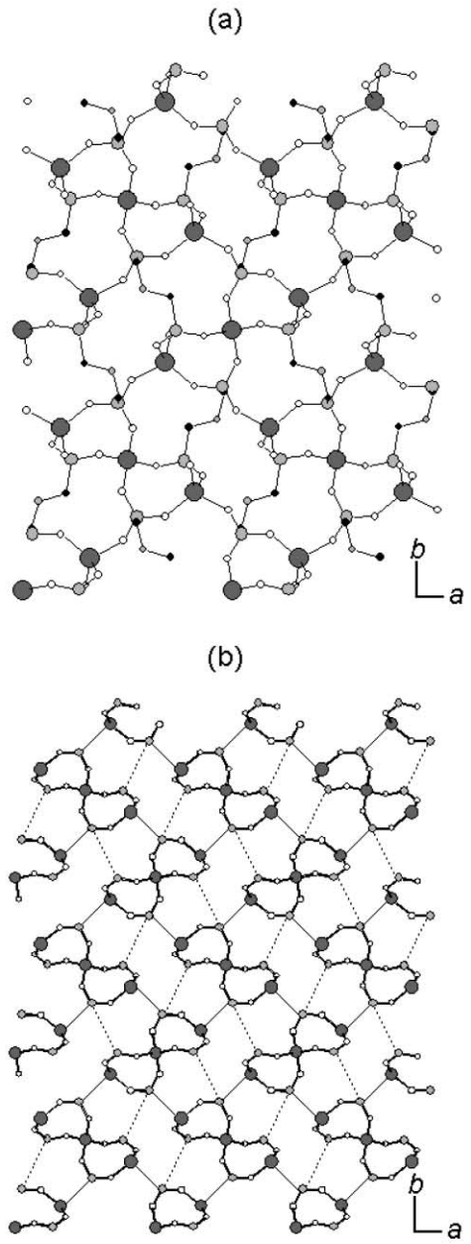

Fig. 1 $Co_3(O_3PCH_2NH_2CH_2PO_3)_2$ viewed along the *c* axis. (a) Ball and stick representation; large dark grey circles are Co atoms, medium light grey circles are P, small black circles are C, small grey circles are N, small white circles are O. H atoms have been omitted for clarity. (b) Schematic view highlighting the way in which the chains are linked *via* $–CH_2NH_2CH_2–$ links (dashed line) and Co–O–P bridges (solid line).

parameters given in Table 1. Bond lengths and selected angles are given in Table 3. The structure is layered and is similar to other layered phosphonate materials in that the layers have an inorganic 'core' with the organic part of the phosphonate anion being directed into the interlayer region (Fig. 3). The similarity with other lamellar divalent metal phosphonates ends at this point.

The layers are based on three crystallographically distinct Co centred octahedra, one CoO_6 (Co3) and two CoO_5N (Co1 and Co2), and two distinct O_3PC tetrahedra. The octahedral co-ordination environments of the Co atoms were confirmed by valence bond calculation, which gave values of 2.020, 1.981 and 1.944 for Co(1), Co(2) and Co(3) respectively. The layers are constructed from pairs of edge-sharing, Co-centred octahedra. Chains are formed in the *b* direction from pairs of Co1 and Co3-centred octahedra. These are linked to one another by corner sharing and through two oxygen atoms of an O_3PC

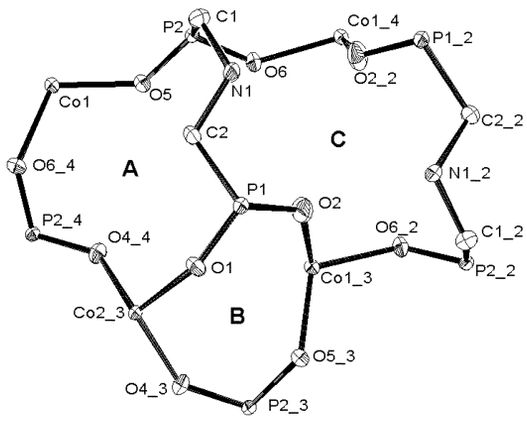

Fig. 2 ORTEP[33] plot of $Co_3(O_3PCH_2NH_2CH_2PO_3)_2$ viewed along the *c* axis, showing the three channel systems. Ellipsoids are 50% probability. Symmetry operations used to generate equivalent atoms: _2 $-x, -y, z$; _3 $-x + 1/2, y + 1/2, -z$; _4 $x + 1/2, -y + 1/2, -z$.

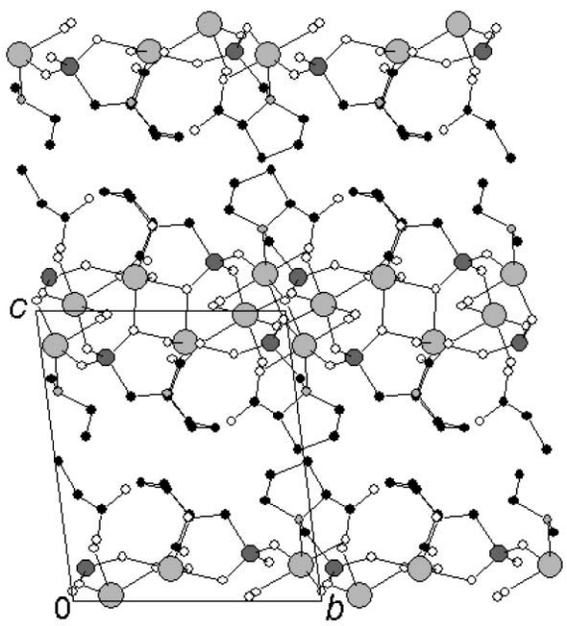

Fig. 3 $Co_3(O_3PCH_2\text{-}NC_4H_7\text{-}CO_2)_2{\cdot}5H_2O$ viewed along the *a* axis, showing the layered nature of the material. Large light grey circles are Co atoms, medium dark grey circles are P, small black circles are C, small grey circles are N, small white circles are O. H atoms have been omitted for clarity.

group. The chains are then connected *via* bridges which are comprised of two O_3PC tetrahedra and another pair of edge shared octahedra (Co2) which can be seen along the *a* axis of the unit cell in Fig. 4. The result of cross-linking the chains in this manner is the formation of rhombohedral chains in the [001] direction. Layered structures containing holes have been observed on numerous occasions in Zn[26,27] and Al phosphates[28] (though the size and shape of the holes differ), but have never been reported for a Co phosphonate to the best of our knowledge.

The octahedra are further held together in the layers by co-ordination from all three of the functional groups, $-PO_3$, CO_2 and $(CH_2)_2NCH_2$, present in the phosphonate anion. Co-ordination of the metal atoms by all of the functional groups present in the phosphonate anions in this manner has been seen before; a similar arrangement is seen in $Al(O_3PCH_2CO_2){\cdot}3H_2O$, where both the phosphate and carboxylate groups are co-ordinated to Al atoms in the same layer.[29] There is then, no cross-linking of layers to result in formation of a three-dimensional porous material. There is, however, a one-dimensional channel system present since the layers are stacked such that the oblique holes are aligned directly above one another in the *c* direction. This channel is, however, small and does not really offer the potential with respect to any application. Water molecules are located in these channels.

Perhaps, the most unusual aspect of this material is the chirality of the proline-derived phosphonic acid. The acid used in the synthetic procedure is chirally pure. In the product however, this is no longer the case. Half of the phosphonate anions have been inverted and are now present as the *R* enantiomer, *i.e.* the acid has been racemised during the synthetic procedure.

The racemisation of amino acids has reportedly been carried out using a variety of methods, including hydrothermal treatment,[30] heating a solution of the amino acid in the presence of an acid or base,[31] or heating a solution in the presence of metal ions.[32] Given the contents of the reaction mixture used in the preparation of **4**, any or all of these causes could be given as leading to the observed racemisation.

Table 3 Bond lengths [Å] and angles [°] for $Co_3(O_3PCH_2NC_4H_7CO_2)_2{\cdot}5H_2O$ (**4**)

Co1–O14	2.021(5)	P2–O14	1.516(5)
Co1–O5[a]	2.067(5)	P2–O15	1.536(5)
Co1–O7	2.070(5)	P2–O9	1.537(5)
Co1–O6	2.119(5)	P2–C7	1.805(7)
Co1–N1	2.163(6)	O7–C1	1.278(9)
Co1–O5	2.189(5)	O2–C12	1.283(10)
Co2–O12[a]	2.036(5)	N2–C7	1.480(9)
Co2–O2[b]	2.062(5)	N2–C8	1.491(10)
Co2–O9	2.099(5)	N2–C11	1.505(9)
Co2–O1	2.133(6)	N1–C3	1.489(9)
Co2–O9[c]	2.152(5)	N1–C2	1.500(9)
Co2–N2[c]	2.243(6)	N1–C6	1.506(8)
Co3–O11	2.050(5)	O8–C1	1.244(9)
Co3–O15	2.075(5)	C1–C2	1.519(11)
Co3–O17	2.103(5)	C3–C4	1.527(11)
Co3–O16	2.125(5)	C2–C5	1.541(11)
Co3–O15[b]	2.135(5)	C12–O13	1.242(10)
Co3–O7	2.182(5)	C12–C8[d]	1.531(12)
P1–O11[a]	1.511(5)	C11–C10	1.477(12)
P1–O12	1.512(5)	C4–C5	1.517(12)
P1–O5	1.543(5)	C10–C9	1.522(14)
P1–C6	1.834(7)	C8–C12[e]	1.531(12)
O14–Co1–O5[a]	101.94(19)	O1–Co2–N2[c]	99.6(2)
O14–Co1–O7	89.98(19)	O9[c]–Co2–N2[c]	84.0(2)
O5[a]–Co1–O7	91.06(19)	O11–Co3–O15	87.1(2)
O14–Co1–O6	92.7(2)	O11–Co3–O17	94.5(2)
O5[a]–Co1–O6	91.1(2)	O15–Co3–O17	178.2(2)
O7–Co1–O6	176.1(2)	O11–Co3–O16	173.5(2)
O14–Co1–N1	98.7(2)	O15–Co3–O16	86.4(2)
O5[a]–Co1–N1	158.0(2)	O17–Co3–O16	92.0(2)
O7–Co1–N1	81.3(2)	O11–Co3–O15[b]	91.22(19)
O6–Co1–N1	95.5(2)	O15–Co3–O15[b]	82.04(19)
O14–Co1–O5	177.46(19)	O17–Co3–O15[b]	98.5(2)
O5[a]–Co1–O5	79.7(2)	O16–Co3–O15[b]	87.16(19)
O7–Co1–O5	88.00(18)	O11–Co3–O7	95.3(2)
O6–Co1–O5	89.27(19)	O15–Co3–O7	98.08(18)
N1–Co1–O5	79.43(19)	O17–Co3–O7	81.2(2)
O12[a]–Co2–O2	92.5(2)	O16–Co3–O7	86.37(19)
O12[a]–Co2–O9	99.5(2)	O15[b]–Co3–O7	173.51(19)
O2[b]–Co2–O9	90.6(2)	O11[a]–P1–O12	113.4(3)
O12[a]–Co2–O1	90.1(2)	O11[a]–P1–O5	112.8(3)
O2[b]–Co2–O1	177.3(2)	O12–P1–O5	112.2(3)
O9–Co2–O1	89.5(2)	O11[a]–P1–C6	105.8(3)
O12[a]–Co2–O9[c]	170.3(2)	O12–P1–C6	108.4(3)
O2[b]–Co2–O9[c]	97.1(2)	O5–P1–C6	103.4(3)
O9–Co2–O9[c]	78.53(19)	O14–P2–O15	114.4(3)
O1–Co2–O9[c]	80.3(2)	O14–P2–O9	111.7(3)
O12[a]Co2–N2[c]	99.8(2)	O15–P2–O9	111.6(3)
O2[b]–Co2–N2[c]	79.4(2)	O14–P2–C7	111.3(3)
O9–Co2–N2[c]	158.6(2)	O15–P2–C7	104.1(3)

Symmetry operations for equivalent atoms: a $-x, -y + 1, -z + 2$; b $-x, -y + 2, -z + 2$; c $-x + 1, -y + 2, -z + 2$; d $x - 1, y, z$; e $x + 1, y, x$.

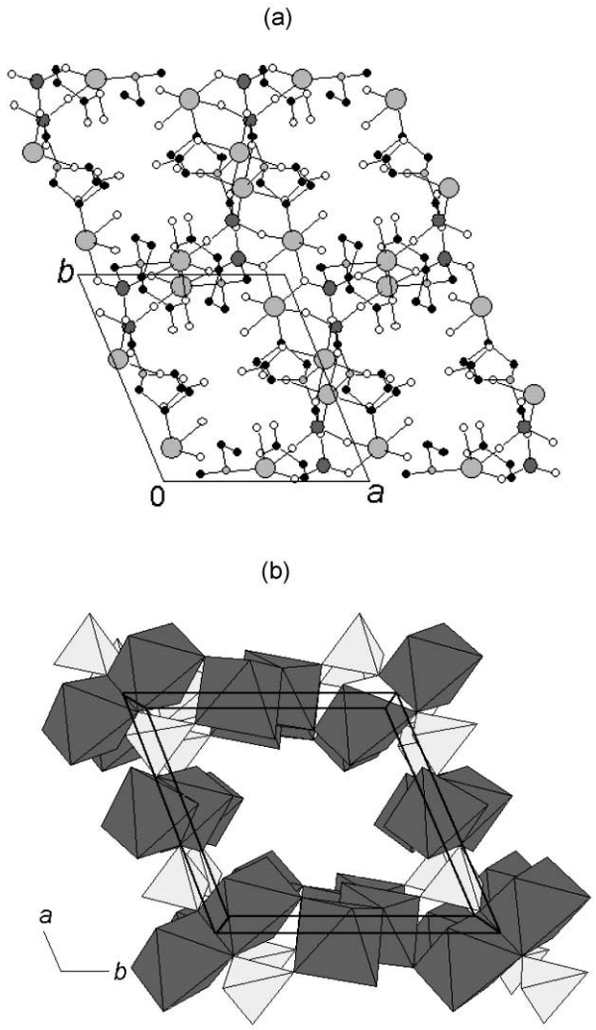

Fig. 4 $Co_3(O_3PCH_2\text{-}NC_4H_7\text{-}CO_2)_2{\cdot}5H_2O$ viewed along the *c* axis, showing rhombohedral holes in the layers. (a) Ball and stick representation showing the proline moeities; large light grey circles are Co atoms, medium dark grey circles are P, small black circles are C, small grey circles are N, small white circles are O. H atoms have been omitted for clarity. (b) Polyhedral view highlighting the connectivity of the pairs of Co-centred octahedra.

The composition of $Co_3(O_3PCH_2\text{-}NC_4H_7\text{-}CO_2)_2{\cdot}5H_2O$ derived from the single crystal data analysis is consistent with the CHN analysis results of the bulk sample (see Experimental section).

Conclusions

Two cobalt phosphonates have been synthesised using trifunctional phosphonate anions with a view to preparing porous materials that contain a 'free' functional group that can be used for some application.

In the case of (**3**), $Co_3(O_3PCH_2NH_2CH_2PO_3)_2$, the synthesis successfully produced a porous material. The structure is formed by interactions between the Co atoms and the phosphate groups, leaving the protonated amine free in one of the three parallel channel systems. The different channel systems are defined by windows of different sizes, however there is no direct correlation between the number of atoms forming the window and the channel diameter. This material is a good candidate for study with respect to ion exchange and ionic transport due to the presence of the protonated amine group in one of the channels. The channels are small, and this precludes the possibility of using the material as a heterogeneous acid catalyst, since substrate molecules would be unable to reach the active site. The logical course of action is to investigate the effects of replacing one (or both) methylene group(s) with ethylene groups to increase the effective channel diameter.

The synthesis of (**4**) using a phosphonate anion based on proline (**2**) was a qualified success since it resulted in the formation of a layered material in which the layers possess holes. Channels are formed by stacking of layers such that the holes are above one another. Zinc phosphates with similar structural features have in the past been described as being porous. All three of the functional groups in the phosphonate anion, however, are involved in co-ordination to the metal atoms, hence any potential application involving a non-bonded functional group is lost. One negative aspect of the result arising from the use of the proline-derived phosphonate is that it has become clear that the hydrothermal method employed here is unlikely to prove successful in attempts to synthesise chiral porous materials, since the chirally pure starting reagent is racemised under the synthetic conditions.

The work presented here demonstrates that trifunctional phosphonate anions can successfully be used in the synthesis of porous materials. Whether or not the material might prove useful in some application depends upon how many of the functional groups are involved in co-ordinating to the metal atoms. It is clear from these results that careful consideration of the type, and arrangement of functional groups is required if we are to be able to produce materials with specific chemical properties, and pore sizes and shapes.

Acknowledgements

G. B. H. would like to thank the EPSRC for the provision of a studentship for A. T. The authors would also like to thank University of London CHN Elemental Microanalysis Service for carrying out the CHN analyses.

References

1 S. Yamanaka, M. Matsunaga and M. Hattori, *J. Inorg. Nucl. Chem.*, 1976, **43**, 1343; S. Yamanaka, M. Tsujimoto and M. Tanaka, *J. Inorg. Nucl. Chem.*, 1978, **41**, 605.
2 J. Le Bideau, C. Payen, P. Palvadeau and B. Bujoli, *Inorg. Chem.*, 1994, **33**, 4885.
3 M. B. Dines and P. DiGiacomo, *Polyhedron*, 1982, **1**, 62.
4 M. B. Dines and P. DiGiacomo, *Inorg. Chem*, 1981, **20**, 92; M. B. Dines and P. C. Griffith, *Inorg. Chem.*, 1983, **22**, 567; M. B. Dines, R. E. Cookesy and P. C. Griffith, *Inorg. Chem.*, 1983, **22**, 1003; M. B. Dines and P. C. Griffith, *Polyhedron*, 1983, **2**, 607.
5 A. Clearfield, *Chem. Mater.*, 1998, **10**, 2801.
6 M. Riou-Cavallec, M. Sanselme, N. Guillou and G. Férey, *Inorg. Chem.*, 2001, **40**, 723.
7 P. Rabu, P. Janvier and B. Bujoli, *J. Mater. Chem.*, 1999, **9**, 1323.
8 A. Distler and S. Sevov, *Chem. Commun.*, 1998, 959.
9 S. Drumel, P. Janvier, P. Barboux, M. Bujoli-Doeuff and B. Bujoli, *Inorg. Chem.*, 1995, **34**, 148.
10 S. J. Hartman, E. Todorov, C. Cruz and S. Sevov, *Chem. Commun.*, 2000, 1213.
11 S. Ayyappan, G. Diaz de Delgado, G. Férey and C. N. R. Rao, *J. Chem. Soc., Dalton Trans.*, 1999, 2905.
12 N. Stock, G. D. Stucky and A. K. Cheetham, *Chem. Commun.*, 2000, 2277.
13 A. Cabeza, M. A. G. Aranda and S. Bruque, *J. Mater. Chem.*, 1998, **8**, 2479.
14 N. Stock, S. A. Frey, G. D. Stucky and A. K. Cheetham, *J. Chem. Soc., Dalton Trans.*, 2000, 4292.
15 G. B. Hix, B. M. Kariuki, S. Kitchin and M. Tremayne, *Inorg. Chem.*, 2001, **40**, 1477.
16 G. B. Hix, A. Turner, B. M. Karuiki, M. Tremayne and E. J. MacLean, *J. Mater. Chem.*, 2002, **12**, 3660.
17 S. Drumel, P. Janvier, D. Deniaud and B. Bujoli, *Chem. Commun.*, 1995, 1051.
18 K. Moedritzer and R. R. Irani, *J. Org. Chem.*, 1966, **31**, 1603.
19 P. J. Diel and L. Maier, *Phosphorus, Sulfur Silicon Relat. Elem.*, 1984, **20**, 313.

20 R. J. Cernik, W. Clegg, C. R. A. Catlow, G. Bushnell-Wye, J. V. Flaherty, G. N. Greaves, I. Burrows, D. J. Taylor, S. J. Teat and M. Hamichi, *J. Synchrotron Radiat.*, 1997, **4**, 279; W. Clegg, M. R. J. Elsegood, S. J. Teat, C. Redshaw and V. C. Gibson, *J. Chem. Soc., Dalton Trans.*, 1998, 3037.
21 G. M. Sheldrick, SHELXTL version 5.1, Bruker-AXS, Madison, WI, 1998.
22 SADABS, Bruker AXS Inc., Madison, WI, 2000.
23 G. M. Sheldrick, SHELX-97, Programs for Crystal Structure Analysis (Release 97-2), Institüt für Anorganische Chemie der Universität, University of Göttingen, Germany, 1998.
24 L. J. Farrugia, WINGX, A Windows program for crystal structure analysis, University of Glasgow, Glasgow, 1998.
25 D. Brown and D. Altermatt, *Acta Crystallogr., Sect. B*, 1985, **41**, 244.
26 A. Choudhury, S. Natarajan and C. N. R. Rao, *Inorg. Chem.*, 2000, **39**, 4295.
27 A. Choudhury, S. Natarajan and C. N. R. Rao, *J. Solid State Chem.*, 2001, **157**, 110.
28 A. M. Chippindale, A. R. Cowley, Q. Huo, R. H. Jones, A. D. Law, J. M. Thomas and R. Xu, *J. Chem. Soc., Dalton Trans.*, 1997, 2639.
29 G. B. Hix, D. S. Wragg, P. A. Wright and R. E. Morris, *J. Chem. Soc., Dalton Trans.*, 1998, 3359.
30 I. Sasaji, M. Hara, S. Tatsumi, K. Seki, T. Akashi and K. Ohno, *US Pat.* 3 213 106, 1965.
31 A. Neuberger, in *Advances in Protein Chemistry*, ed. M. L. Anson and J. T. Edsall, Academic Press, New York, 1948, vol. 4, p. 339.
32 D. E. Metzler, M. Ikawa and E. E. Snell, *J. Am. Chem. Soc.*, 1954, **76**, 648; K. Toi, Y. Izumi and S. Akabori, *Bull. Chem. Soc. Jpn.*, 1962, **35**, 1422.
33 M. N. Burnett and C. K. Johnson, ORTEP-III: Oak Ridge Thermal Ellipsoid Plot Program for Crystal Structure Illustrations, Report ORNL-6895, Oak Ridge National Laboratory, Oak Ridge, TN, USA, 1996.